Footprint Catalysis. VI.[1—5] Chiral "Molecular Footprint" Catalytic Cavities Imprinted by a Chiral Template, Bis(*N*-benzyloxycarbonyl-L-alanyl)amine, and Their Stereoselective Catalyses

Kensaku MORIHARA,* Satoko KAWASAKI, Miki KOFUJI, and Toyoshi SHIMADA
Department of Chemistry, Faculty of Science, Nara Women's University, Kitauoyanishi-machi, Nara 630
(Received October 9, 1992)

Chiral "molecular footprint" catalytic cavities were formed on a silica(alumina) gel surface by molecular imprinting with a chiral template, bis(*N*-benzyloxycarbonyl-L-alanyl)amine. These cavities exhibited stereoselective catalyses in the transacylation of the corresponding substrates: L-, D-, and *meso*- forms of bis(benzyloxycarbonyl-alanyl) oxide.

The authors have developed a "molecular imprinting" method for designing solid acid catalysts with tailored substrate specificities.[1—7] Molecular imprinting with a transition state analogue or a reactive intermediate analogue used as a template provides specific adsorption sites, molecular footprints, on the surface of aluminium ion-doped silica gel. These molecular footprints are cavities comprising a Lewis acid site and complementary structures to the template molecules. They can function as specific catalytic sites due to their specific affinities to the templates, and can also stabilize the transition state of the reaction of a corresponding substrate; such affinities lower the activation energy so that they result in specific catalysis, as can be seen in the active sites of natural enzymes[8] and catalytic antibodies.[9,10]

The previous paper of this series[6] reported that chiral "molecular footprint" cavities could be successfully marked using a chiral template, *N*-benzoyl-N^{α}-(benzyloxycarbonyl)-L-alaninamide (Z-L-Ala–NH–Bz), and that they exhibited enzyme-like enantioselective catalysis in the 2,4-dinitrophenolysis of the corresponding mixed anhydride substrates, benzoyl (*N*-benzyloxycarbonyl-L-, and -DL-alanyl) oxides (Z-L- and -DL-Ala–O–Bz). The difficulty encountered in obtaining optically pure D-substrate, however, forced an indirect investigation of the enantioselective catalyses by kinetic means using the L- and DL-forms of mixed anhydrides. The present paper describes direct evidence for enantioselective catalyses over the other chiral "molecular footprint" cavities marked with bis(*N*-benzyloxycarbonyl-L-alanyl)amine, (**1**); they showed different catalytic activities to L-, D-, and *meso*-forms of bis(*N*-benzyloxycarbonyl-alanyl) oxide, (**2**, **3**, **4**).

Experimental

Materials and Methods. All of the materials were of a guaranteed grade of Nacalai Tesque Co., Ltd., if not otherwise specified. The methods were the same as previously described in detail,[1,3] if not specified.

Template, 1: To *N*-benzyloxycarbonyl-L-alaninamide (1.11 g) in anhydrous tetrahydrofuran (20 cm^3) was added sodium hydride of 60% purity (0.2 g, 1 equiv) under vigorous stirring at room temperature. After 2 min, at which time the evolution of hydrogen ceased, **2** (2.14 g, 1 equiv) was added, followed immediately by another portion of sodium hydride (0.2 g). The reaction was continued for an additional 2 h. The reaction mixture was adjusted to pH 7—8 with acetic acid, and concentrated to nearly dryness under reduced pressure below 45°C. The residue was taken up with ethyl acetate. After drying with sodium sulfate, the ethyl acetate layer was concentrated to syrup at below 45°C. The syrup was treated several times with petr. benzine at 70—80°C to remove the by-product (*N*-benzyloxycarbonyl-L-alanine). The syrup turned into a gummy material, which was crystallized from ethyl acetate–petr. benzine, and subsequently recrystallized from ethanol–water. Yield was 20%. Mp 135—137°C. $[\alpha]_D$ −96° (*c* 2 in acetonitrile). IR (KBr) 3294 (N–H), 1682 (amide I), 1531 (amide II), 1455 (CH_3–), 1258 cm^{-1} (amide III). ^1H NMR ($CDCl_3$) δ=1.22 (d, 6H, CH_3–), 4.42 (m, 2H, C–H), 5.01 (s, 2H, CH_2), 7.32 (m, 10H, ArH), 7.64 (d, 2H, CO–NH), 10.81 (s, 1H, CO–NH–CO). (Found: C, 61.70; H, 5.80; N, 9.80%).

Substrates: **2** and **3** were prepared according to the usual condensation procedures[12] with a half equivalent of dicyclohexylcarbodiimide in acetonitrile, respectively. They were recrystallized from chloroform–petr. benzine, and followed from ethanol–water. **2**: Yield, 70%. Mp 122—128°C. (lit,[11] 131°C). IR (KBr) 3310 (N–H), 1822, 1756 (CO–O–CO), 1687 (amide I), 1542 (amide II), 1456 (CH_3–), 1258 (amide III), 1013 cm^{-1}. $[\alpha]_D$ −33° (*c* 2 in acetonitrile). (Found: C, 61.14; H, 5.70; N, 6.42 %). **3**: Yield, 70%. Mp 123—128°C. IR spectrum was identical with that of **2**. $[\alpha]_D$ +31° (*c* 2 in acetonitrile). **4** was prepared from *N*-benzyloxycarbony-DL-alanine by the above-mentioned procedures. Yield, 25%. Mp 144—148°C. IR (KBr) 3335 (N–H), 1826, 1756 (CO–O–CO), 1696 (amide I), 1535 (amide II), 1451 (CH_3–) 1259 (amide III), 1098, 1065, 1016 cm^{-1}. ^1H NMR ($CDCl_3$) δ=1.48 (d, 6H, CH_3–), 4.45 (m, 2H, C–H), 5.11 (s, 4H, CH_2), 5.20 (2H, N–H), 7.25, 7.35 (4H, 6H, ArH). (Found: C, 61.31; H, 5.70; N, 6.52%).

Silica Gel: Merck Kieselgel 60, art. no. 7754, particle size 0.06—0.20 mm, mesh 70—230, was used.

Catalysts: Details concerning the preparation procedures, if not specified, were the same as those previously described:[1] The surface of the silica gel (100 g) was activated by acid hydrolysis (concd HCl, for 4 h) prior to any subsequent doping with aluminium ions (0.2 mol dm^{-3} $AlCl_3$, 25 cm^3, at 80°C for 3 h) and **1** (0.32 g in acetone, at 80°C for 1 week, pH 4.0). After doping and air-drying (for

15 d), the gel was subjected to methanol extraction in order to remove **1**, which yielded the molecular footprint catalytic cavities (hereafter referred to as {**1**}). The control catalyst stemmed from an aluminium ion-doped gel lacking only imprinting with **1** and possessing native Lewis acid sites without any cavity structure. The presence of "molecular footprint" catalytic cavities on the imprinted catalyst, and their absence on the control catalyst were proved, respectively, as being usual by the occurrence of competitive inhibition caused by the rebinding of **1**.[1—7] Catalytic site molarities were determined using a kinetic titration method through irreversible pyridine-poisoning, as previously reported.[3]

Solvent: Acetonitrile was carefully dehydrated by a previously reported method[3] using calcium chloride, phosphorus pentaoxide, calcium hydride, and fractional distillation with a Himpel column, Bp 81—82°C.

Nucleophile: Potassium 2,4-dinitrophenolate, prepared as previously reported,[3] was recrystallized from water. This salt was solubilized into acetonitrile with 1.2 equivalent mol of 18-crown-6. The stock solution of the nucleophile was at a 5.0×10^{-3} mol dm^{-3} concentration.

Kinetic Measurement. The procedures used for kinetic measurements of the catalyzed 2,4-dinitrophenolysis of **2**, **3**, and **4** were the same as those previously reported.[3] To an acetonitrile solution of a substrate equilibrated with the catalyst (30 or 50 mg) at 30°C, was added a nucleophile solution under vigorous stirring to initiate a catalyzed reaction. The initial concentration of the substrate was 0.9—4.5×10^{-3} mol dm^{-3} and that of the nucleophile was 1.67×10^{-4} mol dm^{-3}. Inhibition studies required preequilibrium of the catalyst with an inhibitor in acetonitrile for 30 min before the addition of a substrate. The catalyzed reaction was followed by triple-wavelength spectrophotometry; decrease in optical density of the nucleophile at 400, 430, and 500 nm was recorded at proper intervals. The reaction obeyed pseudo-first-order kinetics with respect to the nucleophile concentration. The pseudo-first-order rate constants, k_{obsd} s, obeyed Michaelis–Menten kinetics with respect to the substrate concentration. The kinetic parameters, K_m, V_{max} ($k_{obsd.max}$) were obtained from the usual double reciprocal plots (Lineweaver–Burk plots), and k_{cat}s were calculated from V_{max} divided by catalytic site molarities per gram.

Results and Discussion

Characterization of Molecular Footprint Catalytic Cavities. No detectable 2,4-dinitrophenolysis reactions of the substrates occurred without catalysts under the reaction conditions employed, which confirmed that these reactions were actually catalyzed. The catalytic site (Lewis acid site) molarities were kinetically titrated using irreversible poisoning of the Lewis acid sites with pyridine (Fig. 1), where 3.34×10^{-5} mol per gram of the control catalyst and 3.13×10^{-5} mol per gram of the catalyst imprinted with **1** were obtained, respectively. A competitive inhibition of large magnitude, caused by rebinding of the original template used in the imprinting, was used as a criterion for the formation of "molecular footprint" catalytic cavities.[1—6] As shown in Fig. 2, a strong competitive

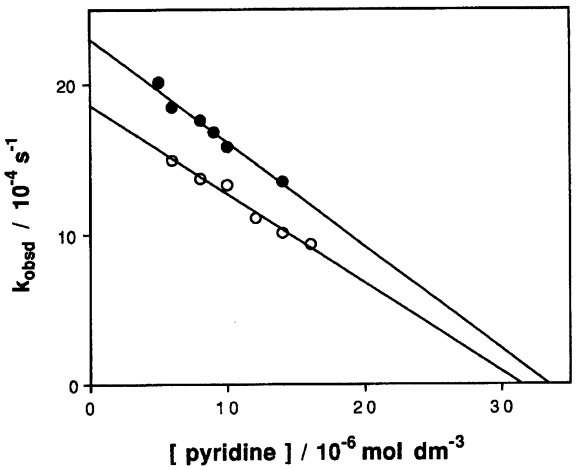

Fig. 1. Catalytic site titrations of the imprinted catalyst and the control catalyst by pyridine poisoning. Substrate (**2**) concentration: 1.8×10^{-3} mol dm^{-3}. Catalyst: 50 mg in 50 cm^{-3} of pyridine–acetonitrile solution. Open circle: The imprinted catalyst, titre; 3.13×10^{-5} mol per 1 gram catalyst. Closed circle: The control catalyst, titre; 3.34×10^{-5} mol per 1 gram catalyst.

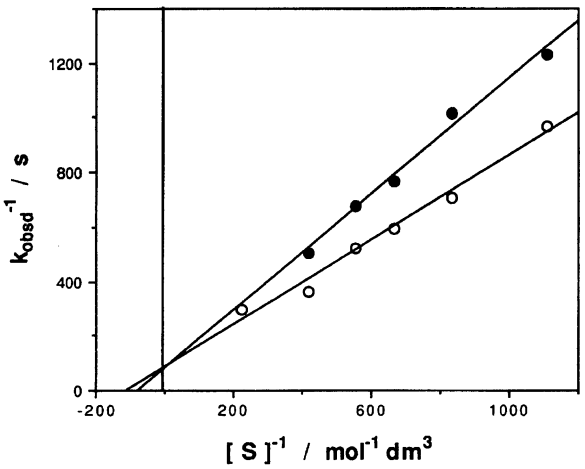

Fig. 2. Competitive inhibition by template **1** on the catalyzed reaction of **2** over the cavities {**1**}. Open circle: No inhibitor **1**. Closed circle: The inhibitor concentration; 1.0×10^{-5} mol dm^{-3}. $K_i=2.22\times10^{-5}$ mol dm^{-3}. $K_m/K_i=411.2$.

inhibition on the {**1**}-catalyzed reaction with **1** ($K_i=2.22\times10^{-5}$ mol dm^{-3}, $K_m/K_i=411.2$), and no inhibition on the control-catalyzed reaction with **1**, undoubtedly proved that the catalytic cavities were successfully formed on the surface, as expected. The obtained kinetic parameters are given in Table 1.

Apparent Stereoselective Catalyses. The native Lewis acid sites of the control catalyst without any cavity structures exhibited no detectable difference in the catalyses among **2**, **3**, and **4**, as shown in Fig. 3. This was because they involved no chiral factor. The catalytic cavities imprinted with **1**, {**1**}, however, dis-

Table 1. Kinetic Parameters of the Catalyzed Reactions over Molecular Footprint Cavities {**1**}

Catalysts	Substrates	K_m[a] 10^{-3} M[f]	V_{max}[b] 10^{-3} M s^{-1}	k_{cat}[c] 10^{3} s^{-1}	k_{cat}/K_m 10^{5} M^{-1} s^{-1}	K_i[d] 10^{-5} M	K_{ip}[e] 10^{-5} M
{**1**}[g]	**2**	9.22 (2.37)[i]	11.90	7.60	8.25 (30.08)	2.22	26.88[h]
{**1**}	**3**	1.66 (1.03)	4.21	2.69	16.15 (26.09)	—	5.79[j]
{**1**}	**4**	6.03 (3.72—7.44)[k]	8.56 (8.56—17.11)	5.47 (5.47—10.94)	9.07 (14.70)	—	
Control[l]	**2**	3.18	3.33	2.00	6.28	No inhibition	
Control	**3**	3.20	3.49	2.09	6.51	—	
Control	**4**	4.45	4.02	2.41	5.41	—	

a) Apparent K_m. b) $k_{obsd.max.}$ with 50 mg catalyst. c) Divided by molarities of catalytic sites of 50 mg catalyst. d) Competitive inhibition constant with the original template **1**. e) K_i of inhibition by reaction products. f) M=mol dm^{-3}. g) Catalytic site molarity; 3.13×10^{-5} mol per 1 gram catalyst. h) K_{iD}. i) Figures in parentheses mean the corrected values. See text. j) K_{iL}. k) Lower and upper limits of parameters. See text. l) Molarity; 3.34×10^{-5} mol per 1 gram catalyst.

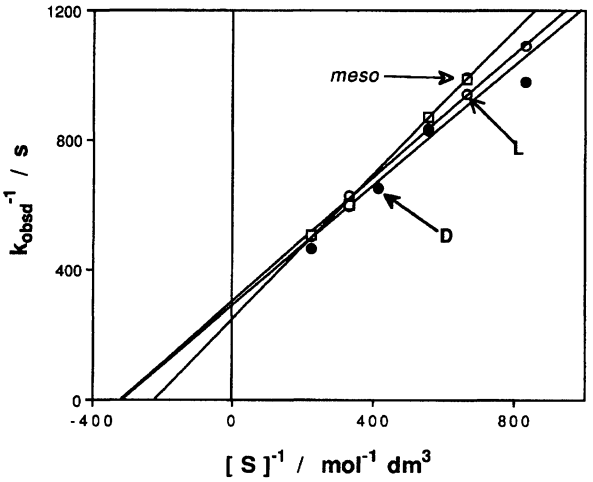

Fig. 3. Lineweaver–Burk plots for the catalyzed reactions of L-, D-, and *meso*-forms of the substrate over the native catalytic sites of the control catalyst. The control catalyst; 50 mg. Open circle for the substrate **2**. Closed circle for **3**. Square for **4**.

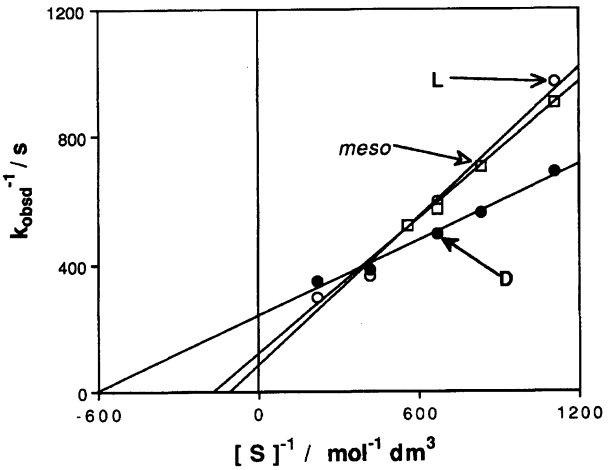

Fig. 4. Lineweaver–Burk plots for the catalyzed reactions of L-, D-, and *meso*-forms of the substrate over the molecular footprint catalytic cavities of the imprinted catalyst {**1**}. The imprinted catalyst; 50 mg. Open circle for the substrate **2**. Closed circle for **3**. Square for **4**.

played distinctly stereoselectie catalyses, as shown in Fig. 4; the reactions of **2**, and **4** were much more effectively catalyzed than that of **3** by factors of nearly 3 and 2, respectively, so far as compared with their V_{max} values (the intercepts on the vertical axis). These evident stereoselective catalyses suggest that certain chiral factor were introduced into the catalytic sites so as to affect the catalytic mechanism. There might be two possibilities for the origin of the chiral factor: Firstly, possible unextracted and still remaining chiral template molecules provide certain chiral effects on the catalysis; secondly, the chiral footprint-like cavities marked with **1** cause chiral effects on the catalysis. Since the abovementioned competitive inhibition with **1** rejects the former because the remaining **1** should act as merely catalytic poison to lose catalytic activity, the latter might be true.

Mechanism of the Stereoselective Catalyses. The observed stereoselective catalyses are complicated. The so-called lock-and-key mechanism based on a simple exclusion effect of the cavities is not likely in this case, since it requires the selectivities to be manifest in the binding steps indicated by the K_m values. The results reveal the apparent selectivities in the catalytic steps indicated by the V_{max} values (Table 1); furthermore, their stereoselectivities vary with the substrate concentration (Fig. 4). These complicated phenomena can be reasonably explained by introducing two assumptions: i) a "productive binding nonproductive binding" mechanism is operating, and ii) competitive inhibition by a product of the reaction occurs.

i) The productive binding and nonproductive binding mechanism had been proposed for certain enzymic catalysis;[13] we introduced it in previous studies in or-

der to explain the enantioselectively catalyzed 2,4-dinitrophenolysis of Z-L- and -DL-Ala–O–Bz over chiral molecular footprint catalytic cavities imprinted with Z-L-Ala–NH–Bz.[6] Knowledge concerning the molecular footprint cavities accumulated so far[2,4,6] suggests that a chiral "molecular footprint" cavity comprises one Lewis acid site (Al atom isomorphically substituted into silicate matrix) and five subsites, as shown in Scheme 1. The five subsites correspond to the partial structures of **1**, respectively, i.e., two subsites correspond to the Z–NH– groups; the other two subsites correspond to methyl-groups (not for α-H); further, one subsite, involving a Lewis acid site within it, corresponds to a carbonyl group of CO–NH–CO. The L-substrate molecule, **2**, might adsorb onto {**1**} with almost the same mode as do the template molecules (**1**) to gain a maximum interaction between **2** and a cavity. Such an adsorption mode, holding the L-configuration at the α-carbon, might place a carbonyl function of CO–O–CO of **2** in contact with a Lewis acid site in the subsite. The acid site can activate the carbonyl function for a subsequent nucleophilic attack with 2,4-dinitrophenolate, which provides an effective catalysis. This constituted "productive binding" (Scheme 2). The D-substrate molecule (**3**), however, might bind onto {**1**} with another adsorption mode. The Z–NH–, and CO–O–CO groups preferentially adsorb onto their corresponding subsites, respectively, because they have a larger interaction than do the methyl groups. In order to maintain the D-configuration of **3**, this adsorption mode forces the methyl groups to move apart from the corresponding subsites, so that they stand perpendicularly. The standing methyl groups shield the carbonyl group attached to a Lewis acid site from any subsequent nucleophilic attack by their steric hindrance, which might result in a less effective catalysis. This constituted "nonproductive binding" (Scheme 2). This mechanism can explain reasonably well the stereoselective catalysis observed among the L-, D-, and *meso*-substrates in the range of high substrate concentrations. The catalytic activities observed in the order L>*meso*>D, reflect the magnitudes of the steric hindrance by **2**, which lacks any standing methyl group, of that by **4** with one standing methyl groups, and of that by **3** with two standing methyl groups, respectively, over the catalytic cavity (Scheme 2).

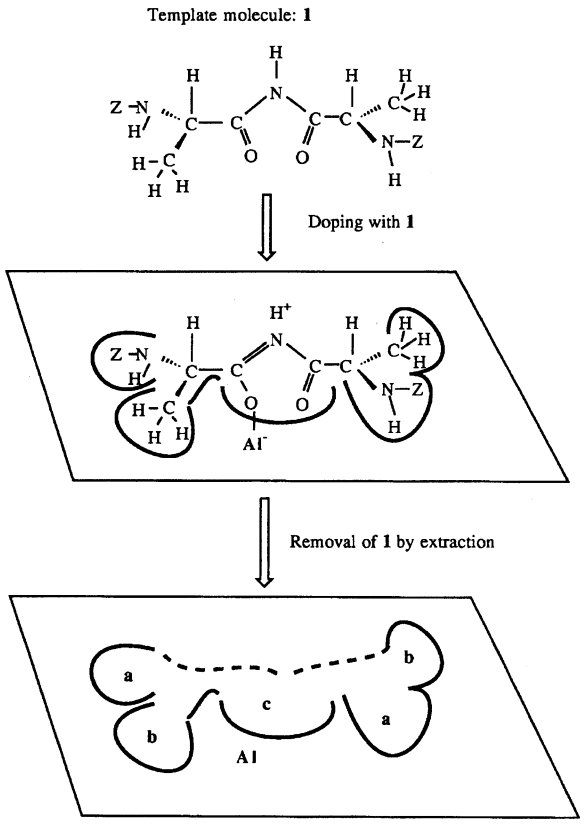

Scheme 1.

ii) The hypothesis, "competitive inhibition by a product of the catalyzed reaction", is proposed to clarify the unexpected inversion of the stereoselectivity. The molecular recognition capabilities of the molecular footprint cavities that reveal catalysis have been confirmed to be the sum of the partial molecular recognition of their subsites.[2] Such partial recognition capabilities, themselves, might provide an inhibitory effect on the catalysis if they have considerable magnitude. One of the catalyzed-reaction products of **2** (Z-L-alaninate, Z-L-NH–CH(–CH_3)–CO–O^-), once released from {**1**}, can bind again on the subsite of {**1**} for an acylamine moiety of **1**, since the product closely resembles the acylamine moiety (Z-L-NH–CH(–CH_3)–CO–N^-–) in molecular shape (Scheme 3). This rebinding should provide competitive inhibition. Similarly, the product of **3** (Z-D-alaninate, Z-D-NH–CH(–CH_3)–CO–O^-) can also rebind on the above-mentioned subsite with a smaller affinity than that of the L-antipode, which would produce a weaker competitive inhibition. Such a potential product inhibition could be qualitatively substantiated by the following inhibition studies. The addition of potassium Z-L-alaninate solubilized with 18-crown-6 on the catalyzed reaction of **3** over {**1**}, and that of potassium Z-D-alaninate on the reaction of **2**, actually displayed typical competitive inhibition plots, respectively, as shown in Figs. 5 and 6. Hence, this hypothesis qualitatively explains the remarkable decrease in the catalytic activity for **2** in the range of low concentration of **2**, which results in an inversion of the stereoselectivity.

Kinetics: According to the above-mentioned mechanisms, the rate law of **2** over {**1**} (Eq. 2), that includes the inhibitory effect by the product, can be derived from the ordinary Michaelis–Menten equation under the pres-

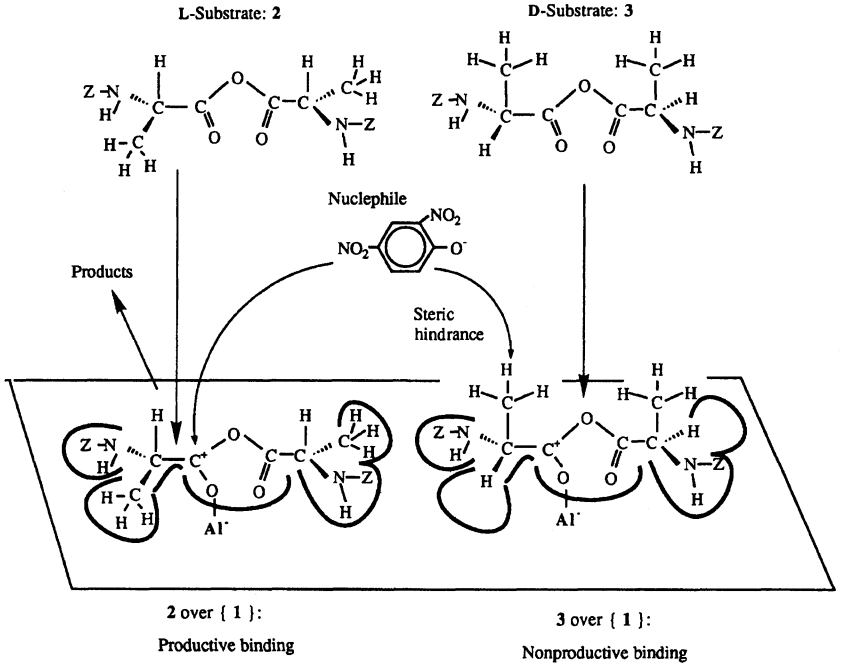

Scheme 2.

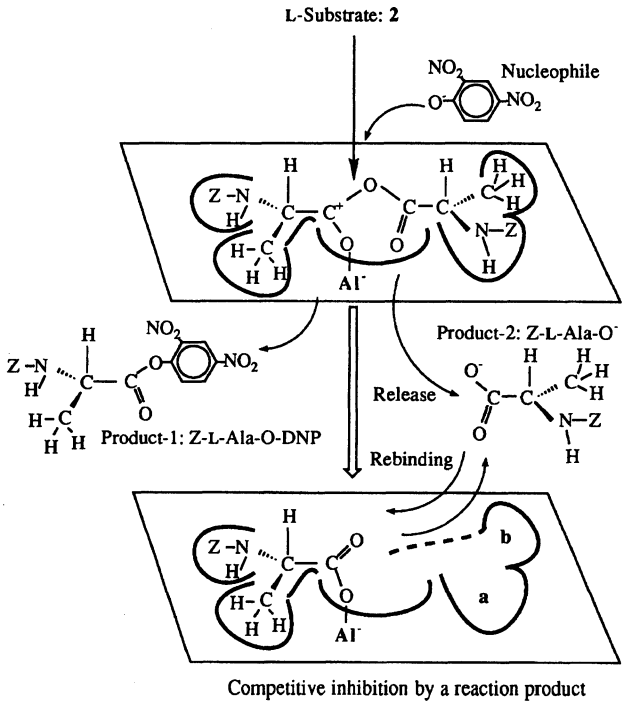

Scheme 3.

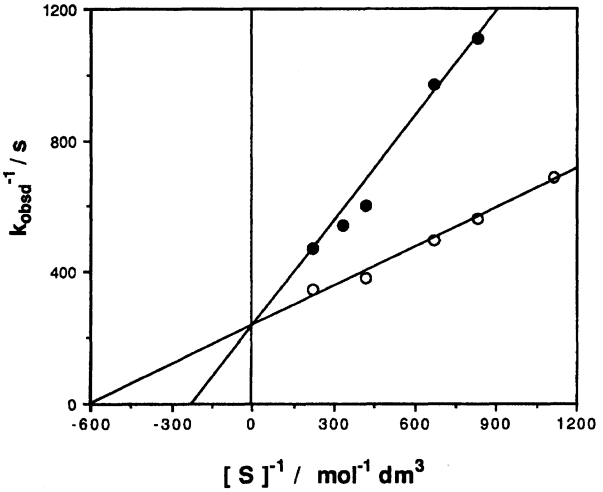

Fig. 5. Competitive inhibition by Z-L-alaninate on the catalyzed reaction of **3** over the cavities {**1**}. Inhibitor: Potasssium Z-L-alaninate solubilized with 18-crown-6. Open circle: No inhibitor. Closed circle: Inhibitor concentration, 1.0×10^{-3} mol dm^{-3}. $K_{iL}=5.795\times10^{-5}$ mol dm^{-3}.

ence of a competitive inhibitor (Eq. 1), as follows:

$$\text{Rate} = \frac{k_{cat}[\text{catalyst}][\text{substrate}]}{K_m\left(1+\frac{[I]}{K_i}\right)+[\text{substrate}]}. \quad (1)$$

Here, [I] is the concentration of the competitive inhibitor in the reaction mixture, and K_i is an competitive inhibition constant between {**1**} and I. Similarly, the following equation can be obtained:

$$k_{obsd} = \frac{k_{cat}[\text{catalyst}][\mathbf{2}]}{K_m\left(1+\frac{[I_L]_t}{K_{iL}}\right)+[\mathbf{2}]}. \quad (2)$$

Here, $[I_L]_t$ is the concentration of the inhibitory product (Z-L-alaninate) at time t, and K_{iL} is the competitive inhibition constant between {**1**} and I_L. The stoichiometry of the reaction requires that the amount of I_L formed by time t should be equal to the amount of consumed nucleophile by time t. Hence, $[I_L]_t$ can be

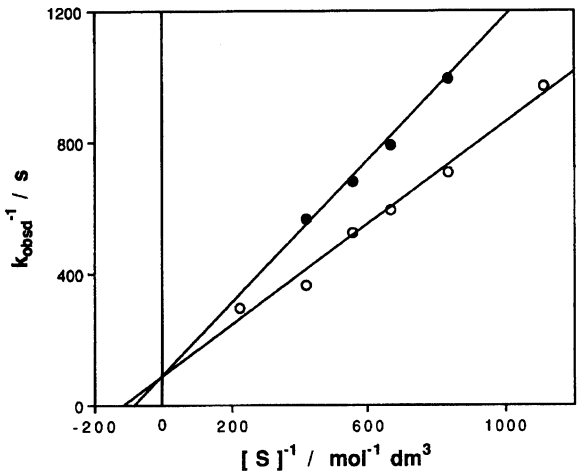

Fig. 6. Competitive inhibition by Z-D-alaninate on the catalyzed reaction of **2** over the cavities {**1**} Inhibitor: Potassium Z-D-alaninate solubilized with 18-crown-6. Open circle: No inhibitor. Closed circle: Inhibitor concentration, 1.0×10^{-3} mol dm^{-3}. $K_{iD}=2.688\times10^{-4}$ mol dm^{-3}.

written as

$$[I_L]_t = [Nu]_0\{1-\exp(-k_{obsd}\times t)\}. \quad (3)$$

Here, $[Nu]_0$ is the initial concentration of the nucleophile. The substitution of Eq. 3 into Eq. 2 gives

$$k_{obsd} = \frac{k_{cat}[catalyst][\mathbf{2}]}{K_m\left(1+\frac{[Nu]_0\{1-\exp(-k_{obsd}\times t)\}}{K_{iL}}\right)+[\mathbf{2}]}. \quad (4)$$

The magnitude of the k_{obsd} value for **2** over {**1**} and that of t (1000—1600 s) under the usual determination conditions of k_{obsd} makes the $\exp(-k_{obsd}\times t)$ term negligibly smaller than 1, which leads to an $[I_L]$ that is nearly $[Nu]_0$. Therefore, Eq. 4 can be roughly approximated as

$$k_{obsd} = \frac{k_{cat}[catalyst][\mathbf{2}]}{K_m\left(1+\frac{[Nu]_0}{K_{iL}}\right)+[\mathbf{2}]}. \quad (5)$$

A similar derivation leads to the following equation for the k_{obsd} of **3** over {**1**}:

$$k_{obsd} = \frac{k_{cat}[catalyst][\mathbf{3}]}{K_m\left(1+\frac{[Nu]_0}{K_{iD}}\right)+[\mathbf{3}]}. \quad (6)$$

On the other hand, the k_{obsd} for the catalyzed reaction of the *meso*-substrate (**4**) over {**1**} is more complicated to formulate than that for the L-substrate shown as Eq. 2. This is because **4** has two probable adsorption modes: one is such that the Z-L-alanyl moiety of **4** binds onto a subsite with a Lewis acid site to attach to it; another is such that the Z-D-alanyl moiety, on the contrary, binds onto the subsite to attach to the acid site. The former adsorption mode provides catalysis with a intrinsic Michaelis constant (K_{mL}) and a rate constant (k_{catL}) to give the Z-L-alanine 2,4-dinitrophenyl ester and Z-D-alaninate as reaction products; the latter mode, however, provides catalysis with another intrinsic Michaelis constant (K_{mD}) and another rate constant (k_{catD}) to yield Z-D-alanine 2,4-dinitrophenyl ester and Z-L-alaninate. The application of a steady state method to the reaction system derives Eq. 7. This deviation is similar to that of the usual Michaelis–Menten equation for a bi-substrate reaction, wherein reverse reactions can be negligible:

$$k_{obsd} = \frac{k_{catL}[catalyst][\mathbf{4}]}{K_{mL}+\left(1+\frac{K_{mL}}{K_{mD}}\right)[\mathbf{4}]}+\frac{k_{catD}[catalyst][\mathbf{4}]}{K_{mD}+\left(1+\frac{K_{mD}}{K_{mL}}\right)[\mathbf{4}]}. \quad (7)$$

If competitive inhibition by the reaction products (Z-L-, and -D-alaninate) takes place, as in the above-mentioned catalysis, K_{mL} and K_{mD} should be corrected by the factor $(1+[I_L]_t/K_{iL}+[I_D]_t/K_{iD})$, respectively, to give

$$k_{obsd} = \frac{k_{catL}[catalyst][\mathbf{4}]}{K_{mL}\left(1+\frac{[I_L]_t}{K_{iL}}+\frac{[I_D]_t}{K_{iD}}\right)+\left(1+\frac{K_{mL}}{K_{mD}}\right)[\mathbf{4}]} + \frac{k_{catD}[catalyst][\mathbf{4}]}{K_{mD}\left(1+\frac{[I_L]_t}{K_{iL}}+\frac{[I_D]_t}{K_{ID}}\right)+\left(1+\frac{K_{mD}}{K_{mL}}\right)[\mathbf{4}]}. \quad (8)$$

Eq. 8, however, cannot be further simplified, as in the case of Eq. 5. This is because $[I_L]_t$ and $[I_D]_t$ cannot be obtained independently using Eq. 3, though only their sum is available, since the stoichiometry requires that $[I_L]_t+[I_D]_t=[Nu]_0\{1-\exp(-k_{obsd}\times t)\}$.

Corrected Stereoselective Catalyses. Since Eqs. 5 and 6 contain unknown constants (intrinsic K_m s, K_{iL}, K_{iD}), respectively, they cannot be mathematically resolved by themselves. If the unknowns are obtainable separately by other means, however, one could use these equations practically to correct the apparent K_m s and k_{cat} s for their intrinsic values. The inhibition of **3** over {**1**} upon addition of Z-L-alaninate (Fig. 4) should be kinetically represented with an additional $[I_L]/K_{iL}$ term into Eq. 6, as follows:

$$k_{obsd} = \frac{k_{cat}[catalyst][\mathbf{3}]}{K_m\left(1+\frac{[Nu]_0}{K_{iD}}+\frac{[I_L]}{K_{iL}}\right)+[\mathbf{3}]}. \quad (9)$$

The inhibitory effect of the constantly existing I_L might be stronger than the generating I_D, since the magnitudes of $[I_L]$ is of the same order as $[Nu]_0$, and is equal to the final concentration of I_D; K_{iL} can be reasonably assumed to be considerably smaller than K_{iD} in magnitude, since the molecular recognition of the subsite for the Z-L-Ala–N$^-$–moiety in {**1**}might favor I_L more than I_D. This consideration makes the $[Nu]_0/K_{iD}$ term negligible, compared to the $[I_L]/K_{iL}$ term. Then, Eq. 9 becomes equal to Eq. 1 in this case. Thus, the apparent K_i value observed in this inhibition (5.795×10^{-5} mol dm^{-3} in Fig. 5) serves as the K_{iL}. Hence, the apparent K_m divided by $\{1+[I_L]_t/K_{iL}\}$ gives the intrinsic K_m value for **2**, (Table 1). A similar treatment as above

gives the intrinsic K_m for **3** and K_{iD} from the inhibition of **2** over {**1**} with the addition of Z-D-alaninate. Substitutions of these intrinsic K_m s, K_{iL}, and K_{iD} values in Eqs. 5 and 6 correct the k_{obsd} values determined in the catalyses of **2** and **3** over {**1**}, respectively. The correction on the catalyzed reaction of the *meso*-substrate **4** over {**1**} requires a further oversimplification. Figure 4 shows that the double reciprocal plot for **4** maintains good linearity (r=0.994), and that it is nearly identical with that for **2**, as compared with that for **3**; these findings imply that most of the *meso*-molecules take the above-mentioned adsorption mode(a) to yield overwhelmingly Z-D-Ala–O^-. This means that k_{catD} and $[I_L]_t$ are negligible, and the Eq. 8 can be rewritten as

$$k_{obsd} = \frac{k_{catL}[\text{catalyst}][\mathbf{4}]}{K_{mL}\left(1+\frac{[Nu]_0}{K_{iD}}\right)+\left(1+\frac{K_{mL}}{K_{mD}}\right)[\mathbf{4}]}. \quad (10)$$

Since the K_{mL} should lie between zero and K_{mD}, the $(1+K_{mL}/K_{mD})$ term then ranges from 1 to 2. Assuming that the term is 1 or 2, substitution of K_{iD} (2.688×10^{-4} mol dm^{-3}) into Eq. 10 gives both the lower and upper limits of the corrected k_{obsd} and K_{mL} for **4**, respectively. Their Linweaver–Burk plots were replotted in Fig. 7. As can be seen there, an enantioselective catalysis for **2** over **3** is distinctly demonstrated throughout the entire range of the substrate concentrations, though these corrections depend on rather less accurate competitive inhibition constants. This finding proves that the assumptions concerning the above-mentioned mechanism are appropriate, and also that the rough approximations employed during the derivation procedures are reasonable. Although a slightly inversed stereoselectivity is still observed between the reactions for **3** and **4**, this rough correction would be sufficient to prove the postulated catalytic mechanisms at the present stage. A more detailed study concerning the product inhibition phenomena, including that of *meso*-substrate, is now being undertaken.

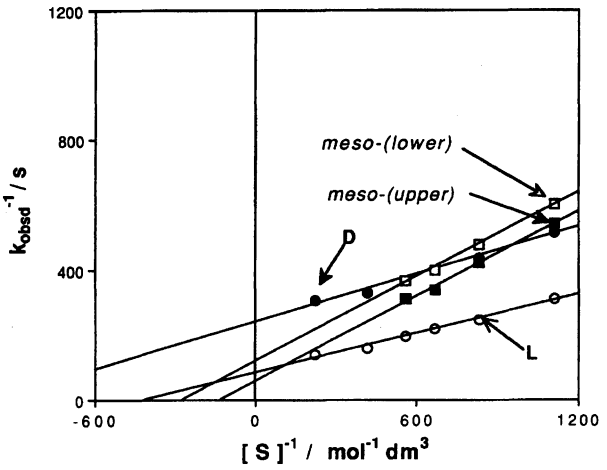

Fig. 7. Corrected Lineweaver–Burk plots for the reactions of L-, D-, and *meso*-forms of the substrate over the cavities {**1**}. Corrected k_{obsd}s are calculated using Eqs. 5, 6, and 10 (see text). Open circle for **2**. Closed circle for **3**. Open square for **4** (lower limit). Closed square for **4** (upper limit).

Conclusive Remarks. The molecular footprint catalytic cavities chirally imprinted displayed unprecedented catalytic features. They evidently exhibited an enzyme-like enantioselective catalysis by a productive binding and nonproductive binding mechanism, as well as by a product inhibition phenomenon. The latter was not caused by the adhesion of the reaction product, as is often observed, but was brought about by rebinding onto the acid site of a reaction product once released from another subsite. Therefore, this inhibitory effect might be referred to as being a most primitive negative feed-back regulation of a catalytic site.[12,13] It should be noted that these catalytic features were spontaneously induced to the catalysts merely by the precise molecular recognition capabilities of the cavities with precise complementary structures to the template; further, the stereoselective catalysis for **4** over {**1**} might result in an asymmetric synthesis wherein an achiral substrate generates chiral products. An application of the asymmetric synthesis with the product-regulation of catalysis to the design of a catalytic system is in progress.

The authors would like to thank Dr. Takashi Nakazawa for his helpful advice and NMR measurements.

References

1) Part I: K. Morihara, S. Kurihara, and J. Suzuki, *Bull. Chem. Soc. Jpn.*, **61**, 3991(1988).
2) Part II: K. Morihara, E. Nishihata, M. Kojima, and S. Miyake, *Bull. Chem. Soc. Jpn.*, **61**, 3999(1988).
3) Part III: K. Morihara, E. Tanaka, Y. Takeuchi, K. Miyazaki, N. Yamamoto, Y. Sagawa, E. Kawamoto, and T. Shimada, *Bull. Chem. Soc. Jpn.*, **62**, 499(1989).
4) Part IV: T. Shimada, K. Nakanishi, and K. Morihara, *Bull. Chem. Soc. Jpn.*, **65**, 954(1992).
5) Part V: T. Shimada, R. Kurazono, and K. Morihara, *Bull. Chem. Soc. Jpn.*, **66**, (1993), in press.
6) K. Morihara, M. Kurokawa, Y. Kamata, and T. Shimada, *J. Chem. Soc., Chem. Commun.*, **1992**, 358.
7) T. Matsuishi, T. Shimada, and K. Morihara, *Chem. Lett.*, **1992**, 1921.
8) L. Pauling, *Chem. Eng. News*, **24**, 1375(1946); *Am. Scient.*, **36**, 51(1948).
9) A. Tramontano, K. D. Janda, and R. A. Lerner, *Proc. Natl. Acad. Sci. U.S.A.*, **83**, 6736(1986).
10) J. Jacob, P. G. Schlutz, R. Sugawara, and M. Powell, *J. Am. Chem. Soc.*, **109**, 2174(1987).
11) T. Wieland, W. Kern, and R. Sehring, *Justus Liebigs Ann. Chem.*, **569**, 122(1950).
12) J. P. Greenstein and M. Winiz, "Chemistry of the Amino Acids," John Wiley & Sons, Inc., New York–London (1961), p. 1016.
13) S. A. Bernhard and H. Gutfreund, "Proc. Intern.

Symp. Enzyme Chem.," Tokyo–Kyoto(1958), p. 124.
14) H. E. Umbarger and B. Brown, *J. Biol. Chem.*, **233**, 415(1958).
15) G. N. Cohen and J. C. Patte, *Cold Spring Harbor Symp. Quant. Biol.*, **6**, 306(1963).